POLISH MARITIME RESEARCH 4 (120) 2023 Vol. 30; pp. 74-80
10.2478/pomr-2023-0060

TRANSFER FUNCTION FOR A CONTROLLABLE PITCH PROPELLER WITH ADDED WATER MASS

Volodimir Leshchev
Igor Maslov
Oleksandr Palagin
Andrii Naydyonov
Department of Ship Power Plants and Systems, Danube Institute of the National University „Odessa Maritime Academy", Ukraine

* Corresponding author: *v.leshchev@ukr.net (V. Leshchev)*

ABSTRACT

The relevance of this study lies in the fact that it presents a mathematical model of the dynamics of the propulsion system of a ship that takes into consideration the mass of water added to it. The influence of this phenomenon on the resonant frequencies of the propeller shaft is examined, and a transfer function for a controllable-pitch propeller is obtained for various operating modes. The purpose of the study is to improve the calculation of the dynamic operating modes of a controllable-pitch propeller by examining the features of a visual models. The VisSim software package is used in the study. A visual model is developed that considers the influence of the rotational speed on the value of the rotational inertia attached to the variable-pitch screw of the mass of water, and a special transfer function is proposed. The study shows that a transfer function of this type has a loop enabling negative feedback. An analysis of the operation of the propeller shaft at its resonant frequency is conducted based on the application of frequency characteristics using the transfer functions obtained. We show that in the low-frequency region, a consideration of the added rotational inertia using the proposed transfer function leads to a significant difference compared to the result obtained with the existing calculation method.

Keywords: propulsion system, torsional vibrations, shaft line, added water mass, transfer function, propeller screw

INTRODUCTION

When calculating the free oscillations that occur in the propeller shaft of a ship, the inertia moment of the controllable pitch propeller (CPP) is usually increased by 20–40% to obtain a match between the calculated results and the experimental ones. Such a solution is not always optimal, since there is a discrepancy between the specified calculated frequencies and the actual ones, especially at low angular speeds of rotation. This means that when calculating the dynamic modes of operation of the propulsion system of a ship, it is necessary to use techniques based on a simplification of the physical process, as reported in [1-5].

One of the existing ways to increase the accuracy of the calculated results compared to those obtained in practice is to search for a solution using a mathematical model based on the construction of a visual image. This issue has been widely covered in a great number of studies. For example, in [6-10], the problems associated with the hydrodynamic interaction between a propeller and water are investigated, and the authors explore how the unevenness of the water flow affects the results of the axial and tangential forces acting on the propeller. However, it is not shown how the resulting harmonic components of the moments of these forces affect

the resonant phenomena in the propulsion complex. In [11-14], the interaction between the propeller and the elements of the ship's hull is investigated, and it is shown that modern computational fluid dynamics solvers can give correct calculation results when the rudder operates in the propeller flow, although these studies rarely consider the features of the dynamics of the propulsion system from the action of the displaced water mass.

The studies in [15-20] explore the dynamics of a ship's propeller when the water surface is agitated using a model that includes an increase in the rotational inertia of the propeller due to the simple addition of the water mass. The difficulty of this approach means that such studies are limited. Thus, despite abundant research in the field of dynamics on the propulsion system of ships, the issue of the features of stability and resonant frequency phenomena in the interaction of the propeller and the aquatic environment remains unresolved.

The purpose of this study is to improve the calculation of the dynamic operating modes of a controllable-pitch propeller by examining the features of a visual model.

MATERIALS AND METHODS

This study involves mathematical modelling of the process that occurs during the movement of the ship, that is, the interaction between a controllable-pitch propeller and the aquatic environment for a propulsion system represented in the form of a three-mass mechanical system (TMS) [21]. In this approach, three distinct masses represent integral components of the propulsion pathway. The first mass corresponds to the diesel engine, and includes its rotational inertia and the torque it produces. The intermediary mass represents the gearbox or reduction gear, and accounts for its rotational inertia and its role in moderating the engine speed for the propeller. The final mass represents the propeller and its shaft, and includes the propeller's rotational inertia and the resistance it faces due to water and other factors. The VisSim software package is used here to visualise the results of the study. VisSim is a visual-based block diagram programming language tailored for simulation and embedded system development. It has been extensively employed in the design of control systems and digital signal processing, and facilitates multi-domain design and simulation. The language offers blocks for arithmetic, Boolean, and transcendental operations, in addition to digital filters, transfer functions, numerical integration, and interactive graph plotting [22]. Figure 1 shows a model diagram of the TMS of a ship's propulsion system [17, 22], with a modified transmission function for the CPP in accordance with the one proposed in this study.

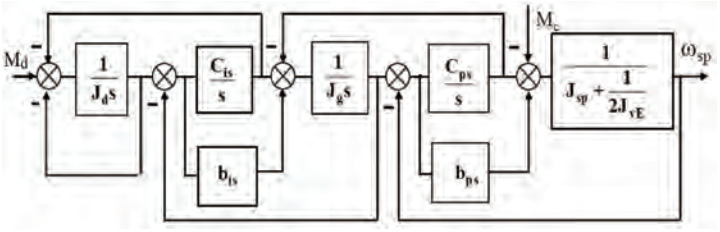

Figure 1. Model of the three-mass mechanical part of the propulsion system (M_d – torque produced by the diesel engine, M_c – resistance torque on the propeller shaft, J_d, J_g, J_{sp} – rotational inertia of the engine, gearbox, and propeller respectively, C_{is} – stiffness of the intermediate shaft, C_{ps} – stiffness of the propeller shaft, b_{is}, b_{ps} – viscous friction coefficients for the shafts, s – differentiation operator)

Table 1 shows the designations of the model elements used in the study and their given values. The angular velocities of the rotating elements of the propulsion system, after being connected to the motor shaft, are assumed to be equal:

$$\omega_d = \omega_{is} = \omega_{ps} = \omega_{sp} = 1 \quad (1)$$

All values of frequencies and angular velocities in the text and figures are given in rad·s^{-1} due to the limitations of the VisSim software product.

Table 1. Designations and technical parameters of the ship's propulsion system

Elements of the propulsion system of the ship	Symbol	Parameter values before casting	Parameter values after casting
Diesel rotational inertia	J_d	4.50·10^3 kg. m^2	4.50kg. m^2
Rotational inertia of the gearbox	J_r	2.40·10^3 kg. m^2	0.24kg. m^2
Estimated rotational inertia of the screw	J_{sp}	3.2·10^3 kg. m^2	0.32kg. m^2
Rotational inertia of the added water	J_v=(0.2-0.4)J_{sp}	(0.6-1.2)·10^3 kg. m^2	(0.6-0.12)kg. m^2
Stiffness of the intermediate shaft	C_{is}	0.64·10^6 N.m	0.64N.m
Stiffness of the propeller shaft	C_{ps}	0.24×10^6 N.m	0.024N.m
Gear ratio of the gearbox	i_g	3.19	3.19
Nominal angular rotation speed of the diesel engine	ω_{dn}	40.317rad·s^{-1}	1

Since the action of the dissipative forces of the viscous action is assumed to be equal to zero, the values of the resonant frequencies in the shaft line obtained from experiment are close to the calculated values [22]. The study was conducted using the VisSim experimental setup shown in Figure 2. In addition to the TMS, the model shown in Figure 2 also contains an exciting scanning signal generator (SSG) [17].

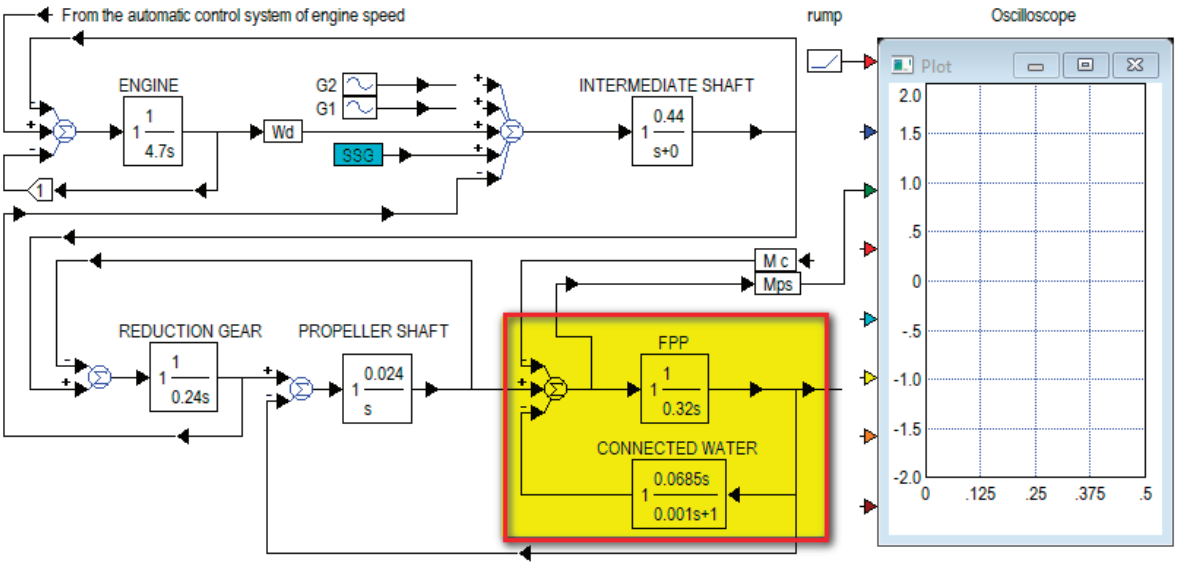

Figure 2. Diagram of the dynamic model of the three-mass mechanical part of the propulsion system of the ship

This generator supplies the diesel output with a sinusoidal signal with a constant amplitude and frequency, which varies in proportion to time with acceleration $\varepsilon_\omega = 0.001 \text{rad/s}^2$. This signal simulates the rotation of the diesel engine, which leads to resonant phenomena in the shaft line.

The operation of the model and the interaction of its parts are described in [22]. Fixed frequency generators G1 and G2 are designed to check and refine the values found during scanning of the critical frequencies Ω_{cr1} and Ω_{cr2}. The experimental equipment for the study was provided by the Danube Institute of the Odessa Maritime Academy.

RESULTS AND DISCUSSION

It is known that in a ship's propulsion system, a fixed-pitch propeller (FPP) under ideal conditions, taking into account the slippage of the propeller blades relative to the water, displaces and swirls a unit mass of attached water per one revolution:

$$m_{vE} = \pi\rho\frac{D_{sp}^2}{4}(1-\alpha)H_{sp}, \tag{2}$$

where m_{vE} is the unit mass of the added water formed from one turn of the screw; H_{sp} is the pitch of the propeller; D_{sp} is the diameter of the propeller; ρ is the density of water; and α is the coefficient of sliding.

When using the above units, the angular frequency of a rotation and the rotational speed are related by the expression:

$$n_{sp} = \frac{\omega_{sp}}{2\pi} \tag{3}$$

The mass of the added water jet m_v at the rotational speed of the propeller ω_{sp}(rad/s) can then be represented by the formula:

$$\begin{aligned} m_v = m_{vE}n_{sp} = \pi\rho\frac{D_{sp}^2}{4}(1-\alpha)H_{sp}\frac{\omega_{sp}}{2\pi} = \\ = \frac{1}{8}\rho D_{sp}^2(1-\alpha)H_{sp}\omega_{sp}, \end{aligned} \tag{4}$$

where n is the speed of rotation of the propeller, and ω_{sp} is its rotational speed (rad/s).

If the rotating mass of water is a full-bodied cylinder with radius:

$$R_v = \frac{D_{sp}}{2}, \tag{5}$$

then, from Eq. (4), the following can be obtained:

$$\begin{aligned} J_v(t) = \frac{1}{2}\pi R_v^2 m_v(t) = \\ = \frac{1}{64}\pi\rho D_{sp}^4(1-\alpha)H_{sp}(t)\omega_{sp}(t). \end{aligned} \tag{6}$$

In the existing method of dynamic calculation, the problem of finding the moment:

$$J_\Sigma = \mathrm{J_{sp}} + \mathrm{J}_v \tag{7}$$

is reduced to simply increasing it by 20–40% of the calculated value:

$$J_\Sigma = (1.2-1.4)J_{\mathrm{sp}} \tag{8}$$

This allows for some coincidence between the results of the calculation of critical frequencies with their real values. However, it follows from Eq. (6) that the moment J_v is not constant, but changes over time depending on the changes of the variable components $\omega_{sp}(t)$ and $H_{sp}(t)$. The dynamics equation for the screw in this case takes the form:

$$M_{ps}(t) = \frac{d}{dt}\left[J_{\Sigma}\left(H_{sp}(t), \omega_{sp}(t)\right)\right]$$
$$= \frac{d}{dt}\left[J_{sp}\omega_{sp}(t) + \left(\frac{1}{64}(1-\alpha)\pi\rho D_{sp}^4\right)H_{sp}(t)\omega_{sp}^2(t)\right] =$$
$$= J_{sp}\frac{d\omega_{sp}}{dt} + \left(\frac{1}{64}(1-\alpha)\pi\rho D_{sp}^4\right)\frac{d}{dt}\left[H_{sp}(t)\omega_{sp}^2(t)\right] =$$
$$= J_{sp}\frac{d\omega_{sp}}{dt} + J_v\frac{d}{dt}\left[H_{sp}(t)\omega_{sp}^2(t)\right]. \quad (9)$$

The second part of Eq. (9) represents the torque of the displaced water mass M_v, which contains the differential of the product of the variables H(t) and $\omega_{sp}(t)$. This product is differentiated as follows:

$$\frac{d}{dt}\left(H_{sp}\omega_{sp}^2\right) = 2H_{sp}\omega_{sp}\frac{d\omega_{sp}}{dt} + \omega_{sp}^2\frac{dH_{sp}}{dt}. \quad (10)$$

If the expression in Eq. (10) is substituted into Eq. (9), then we have:

$$M_{ps} = J_{sp}\frac{d\omega_{sp}}{dt} + 2\left(\frac{1}{64}(1-\alpha)\pi\rho D_{sp}^4\right)H_{sp}\omega_{sp}\frac{d\omega_{sp}}{dt} + \left(\frac{1}{64}(1-\alpha)\pi\rho D_{sp}^4\right)\omega_{sp}^2\frac{dH_{sp}}{dt}. \quad (11)$$

The terms of this equation by derivatives after grouping are:

$$M_{ps} = \left[J_{sp} + 2\left(\frac{1}{64}(1-\alpha)\pi\rho D_{sp}^4\right)H_{sp}\omega_{sp}\right]\frac{d\omega_{sp}}{dt} + \left(\frac{1}{64}(1-\alpha)\pi\rho D_{sp}^4\right)\omega_{sp}^2\frac{dH_{sp}}{dt}. \quad (12)$$

This expression for the moment M_{ps} holds both for a unit with an FPP and for a unit with a CPP. It describes a single dynamic process that occurs when both accelerating or decelerating $\omega_{ps}(t)$, and when changing the step $H_{sp}(t)$ towards an increase or decrease. There is also a scenario where these two cases act simultaneously. In this study, we investigate the option in which the ship has FPP or a CPP that operates with a given fixed step H_{sp}. Eq. (12) then takes the form:

$$M_{ps} = \left[J_{sp} + 2\left(\frac{1}{64}(1-\alpha)\pi\rho D_{sp}^4\right)H_{sp}\omega_{sp}\right]\frac{d\omega_{sp}}{dt}, \quad (13)$$

where M_{ps} is the torque of the propeller shaft with the FPP.

Part of the second term in Eq. (13) can be interpreted as the rotational inertia of the added water for one revolution of the propeller, and is expressed by the formula:

$$J_{vE} = \left(\frac{1}{64}(1-\alpha)\pi\rho D_{sp}^4\right)H_{sp}. \quad (14)$$

Considering the damping effect of water, we can write Eq. (13) with respect to the rotational inertia of the propeller J_{sp} as follows:

$$M_{ps}(t) - 2J_{vE}\omega_{sp}\frac{d\omega_{sp}}{dt} = J_{sp}\frac{d\omega_{sp}}{dt} \quad (15)$$

Then, the equation for the propeller dynamics takes the form:

$$M_{ps}(t) - M_v(t) = J_{sp}\frac{d\omega_{sp}(t)}{dt}, \quad (16)$$

where $M_v(t) = 2J_{vE}\omega_{sp}(t)d\omega_{sp}(t)\frac{d\omega_{sp}(t)}{dt}$ is the torque from the water added to the propeller.

If we assume that the moment of the load $M_c(s) = 0$ then under zero initial conditions of the dynamic process, Eq. (16) in the operator form is:

$$M_{ps}(s) - 2J_{vE}\frac{1}{s^2}s = M_{ps}(s) - 2J_{vE}\frac{1}{s} = M_{ps}(s) - M_v(s) = J_{sp}s, \quad (17)$$

where s is the Laplace operator.

Since the propeller is affected by two torques, $M_{ps}(s)$ and $M_v(s)$, the mathematical model of this interaction takes the form shown in Figure 3.

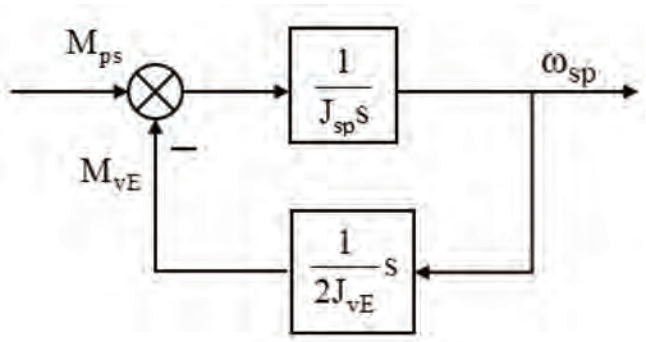

Figure 3. Diagram of the mathematical model of the dynamic interaction between torque and a unit moment

In the diagram of the propulsion system model in Figure 2, this node is highlighted in colour. It contains the values of the elements that correspond to numerical experiment. As can be seen from Figure 3, the moments J_{sp} and J_{vE} are combined into a loop containing negative feedback. The total transfer function of the FPP $W_{sp}^{\Sigma}(s)$ can be then presented in generalised form as:

$$W_{sp}^{\Sigma}(s) = \frac{W_{sp}(s)}{1+W_{sp}(s)W_{vo}(s)} = \frac{\frac{1}{J_{sp}s}}{1+\frac{1}{J_{sp}s^2J_{vE}}} = \frac{1}{\left(J_{sp}+\frac{1}{2J_{vE}}\right)s}. \quad (18)$$

It follows from Eq. (18) that the model of the total transfer function of the propeller $W_{sp}^{\Sigma}(s)$ has the form shown in Figure 4.

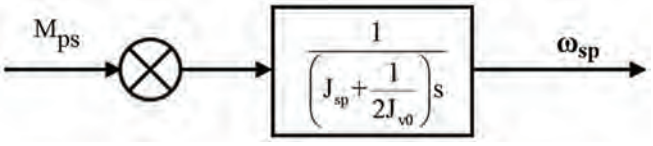

Figure 4. Model of the generalised transfer function of the CPP $W_{sp}^{\Sigma}(s)$ considering the added water mass

The transfer function of the FPP $W_{sp}^{\Sigma}(s)$ found here differs significantly from the one used today in practice, which is accepted as:

$$W_{\text{sp}} = \frac{1}{(1.2\text{-}1.4)J_{\text{sp}}}. \quad (19)$$

It can also be seen from Eq. (18) that the value J_{vE} is specific to each case, and is subject to calculation. The moment J_v is inversely proportional to the unit moment J_{vE}. It follows from this that with a decrease in the step ratio

$$\lambda_{sp} = \frac{H_{sp}}{D_{sp}}, \quad (20)$$

the critical frequency Ω_{cr1} shifts downwards. For a TMS propulsion system, this displacement mainly affects low rotational speeds, and may go beyond the range that corresponds to (1.2 - 1.4) J_{sp}. When calculating the dynamic modes, attention should be paid to this phenomenon. A numerical experiment is conducted with a dynamic model as shown in Figure 2, where the values of the elements of this model are shown in the diagram in accordance with Table 1. Descriptions of the interaction between the parts of the model are presented in [23-26]. For example, the propulsion system of the ship is taken as an FPP with the following technical characteristics: step ratio λ_{sp} = 1.045; coefficient of relative slip α = 0.14; screw diameter D_{sp} = 1.1 m; and engine 6NVD 48A-2U with rated power 852 kW (1158.4 hp), rated engine speed n_{dn} = 385 rpm, and rated speed of the propeller shaft n_{sp} = 118 rpm. A comparative analysis of the dynamics of the propulsion system is conducted for three scenarios. In the first, the FPP has an estimated rotational inertia of

$$J_{\text{sp1}} = 3.20 \text{ kg} \cdot m^2, \quad (21)$$

and in the second, the FPP has a rotational inertia that is increased by 40%:

$$J_{\text{sp2}} = 4.48 \text{ kg} \cdot \text{m}^2. \quad (22)$$

The third involves a screw with a rotational inertia determined using the method proposed in this study in accordance with Eq. (18). The unit moment J_{vE} is calculated by Eq. (2), where the screw pitch H_{sp} is replaced by a step ratio λ_{sp}. Then, for ω_{spn} = 1, Eq. (2) becomes:

$$J_{vE} = \frac{1}{64}\pi\rho D_{sp}^5(1-\alpha)\lambda_{sp}k_g, \quad (23)$$

where $k_g = \frac{1}{i^2}$ is the moment reduction coefficient.

By substituting the values of the circuit elements (Table 1) into Eq. (23), the following estimate can be obtained:

$$J_{vE} = \frac{1}{64}\pi \cdot 1.025 \cdot 1.1^5 \cdot (1-0.14) \cdot 1.045 \cdot 0.10 \simeq \simeq 0.0073 \text{ t} \cdot m^2 = 7.30 \text{ kg} \cdot m^2 \quad (24)$$

The transfer function of the added moment W_v then takes the value:

$$W_v = \frac{1}{2J_{vE}}s = \frac{1}{2 \cdot 7{,}30}s = 0.0685s. \quad (25)$$

The transfer function $W_v(s)$ is implemented as a typical differentiating link:

$$W_v(s) = \frac{T_1 s}{T_2 s+1} = \frac{0.0685s}{0.001s+1}. \quad (26)$$

The total value of the moment J_Σ in this case is equal to:

$$J_\Sigma = J_{sp} + \frac{1}{2J_{vE}} = 0.32 + 0.0685 = = 0.3885\text{кг} \cdot m^2. \quad (27)$$

After modelling the dynamic process, the critical frequencies are found by scanning the model with the SSG variable signal generator for the three variants, and have the following values: $\Omega_{\text{cr1-1}}$ = 0.2081rad*s^{-1}, $\Omega_{\text{cr1-2}}$ = 0.22329rad*s^{-1}, $\Omega_{\text{cr1-3}}$ = 0.2603rad*s^{-1}, $\Omega_{\text{cr2-1}} = \Omega_{\text{cr2-2}} = \Omega_{\text{cr2-3}}$ = 1.4332rad*s^{-1}.

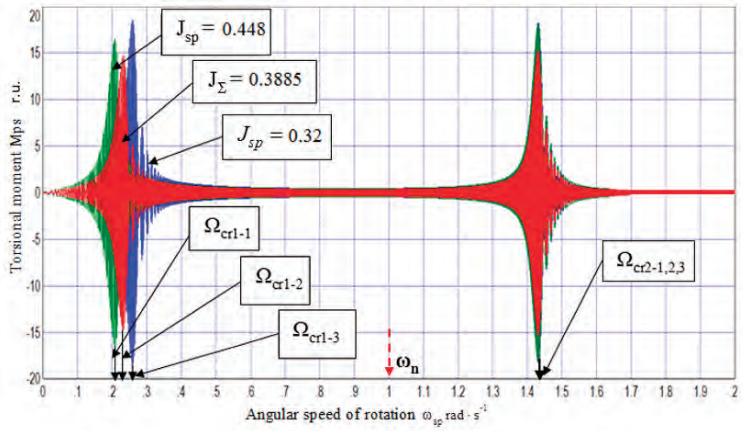

Figure 5. Critical frequencies of the torque $\Omega_{cr1\text{-}1}$, $\Omega_{cr1\text{-}2}$, and $\Omega_{cr1\text{-}3}$ for the TMS propulsion system for various values of the moment J_v

As can be observed from the oscillogram in Figure 5, the high critical frequencies of the torque , $\Omega_{\text{cr2-1}}$, $\Omega_{\text{cr2-2}}$ and $\Omega_{\text{cr2-3}}$ are almost the same. This allows us to conclude that the rotational inertia of displaced water J_v has little effect on critical frequencies that occur below the maximum engine speed [27-31].

CONCLUSION

Our results show that for the propulsion system considered here, the critical frequency $\Omega_{\text{cr1-2}}$ obtained using the propeller transfer function proposed in this study is within the existing range of changes in critical frequencies, which are typically estimated in practice by increasing the moment J_{sp} by 20–40%. It corresponds to a total moment J_{sp} = 0.3885 kg · m^2, which represents an increase of 21.9% and confirms the validity of its application. The proposed method for determining the rotational inertia of a screw with a displaced water mass allows us to calculate the ratio directly, without the need for approximate empirical formulae such as Kutuzov's formula,

which does not consider the dependence of the moment J_v on the rotation frequency of the mass of the water jet.

A visual dynamic model was developed that considered the influence of the rotational speed on the value of the rotational inertia of water mass added to the CPP, and a special transfer function for the propeller was proposed. It was established that such a transfer function has a loop with negative feedback. The operation of the ship's shaft line when using the proposed transfer functions in the model of the propulsion system was explored. An analysis of the resonant modes based on the application of frequency characteristics using the transfer functions obtained in the study was conducted. It was found that when determining the critical oscillation frequencies of the shaft line in the lower part of the propeller operating range, considering the added moment leads to a significant difference compared to the results obtained from the existing method.

NOMENCLATURE

CPP	Controllable-pitch propeller
FPP	Fixed-pitch propeller
SSG	Scanning signal generator
TMS	Three-mass mechanical system

REFERENCES

1. MacPherson, D.M., Puleo, V.R., Packard, M.B. 2007. Estimation of entrained water added mass properties for vibration analysis. https://cutt.ly/8GVZdOe.

2. Faltinsen, O., Minsaas, K.J., Liapias, N., Skjørdal, S.O. 1981. Prediction of resistance and propulsion of a ship in a seaway. In: T. Inui (Ed.). Proceedings of 13th Symposium on Naval Hydrodynamics (pp. 1-19). Tokio: University of Trondheim.

3. Król, P. 2021. Hydrodynamic state of art review: Rotor – stator marine propulsor systems design. Polish Maritime Research, 28(1), 72-82. https://doi.org/10.2478/pomr-2021-0007

4. Koibakov, S.M., Umirkhanov, M.G. 2013. Model research of ice jams. World Applied Sciences Journal, 25(8), 1158-1160. https://doi.org/10.5829/idosi.wasj.2013.25.08.13382

5. Koibakov, S.M., Umirkhanov, M.G. 2013. Icebreaker unit. World Applied Sciences Journal, 25(8), 1251-1254. https://doi.org/10.5829/idosi.wasj.2013.25.08.13423

6. Gayen, D., Chakraborty, D., Tiwari, R. 2017. Whirl frequencies and critical speeds of a rotor-bearing system with a cracked functionally graded shaft – finite element analysis. European Journal of Mechanics – A/Solids, 61, 47-58.

7. Lou, B., Cui, H. 2021. Fluid–structure interaction vibration experiments and numerical verification of a real marine propeller. Polish Maritime Research, 28(3), 61-75. https://doi.org/10.2478/pomr-2021-0034

8. Prohl, M.A. 1945. A general method for calculating critical speeds of flexible rotors. Journal of Applied Mechanics, 12(3), 142-148.

9. Ostanin, V. 2022. Vadym Effects of repulsion and attraction between rotating cylinders in fluids. Scientific Herald of Uzhhorod University. Series "Physics", (51), 39-47. https://doi.org/10.54919/2415-8038.2022.51.39-47

10. Klendii, M., Logusch, I., Dragan, A., Tsvartazkii, I., Grabar, A. 2022. Justification and calculation of design and strength parameters of screw loaders. Machinery & Energetics, 13(4), 48-59. https://doi.org/10.31548/machenergy.13(4).2022.48-59

11. Yoon, M. 2016. A Transfer Function Model of Thrust Dynamics for Multi-Rotor Helicopters. International Journal of Engineering Research & Technology, 5(1), 15-18.

12. Boletis, E., de Lange, R., Bulten, N. 2015. Impact of propulsion system integration and controls on the vessel DP and maneuvering capability. IFAC-PapersOnLine, 48(16), 160-165.

13. Xiros, N.I. 2004. PID marine engine speed regulation under full load conditions for sensitivity H∞-norm specifications against propeller disturbance. Journal of Marine Engineering & Technology, 3(2), 3-11.

14. Smailova, G., Yussupova, S., Uderbaeva, A., Kurmangaliyeva, L., Balbayev, G., Zhauyt, A. 2018. Calculation and construction of the tolling roller table. Vibroengineering Procedia, 18, 14-19. https://doi.org/10.21595/vp.2018.19908

15. Koushan, K. 2006. Dynamics of ventilated propeller blade loading on thrusters. In: World Maritime Technology Conference (pp. 18-21). London: Macmillan Education.

16. Senjanović, I., Hadžić, N., Murawski, L., Vladimir, N. 2019. Analytical procedures for torsional vibration analysis of ship power transmission system. Engineering Structures, 178, 227-244.

17. Leschev, V.A. 2018. Marine diesel ACS with external feedback speed sensor. Modern Engineering and Innovative Technologies, 5, 11-17.

18. Kukhar, V., Vasylevskyi, O., Khliestova, O., Berestovoi, I., Balalayeva, E. 2022. Hydraulic Press Open Die Forging of 21CrMoV5-7 Steel CCM Roller with Flat Upper and Concave Semi-round Lower Cogging Dies. Lecture Notes in Mechanical Engineering, 489-498. https://doi.org/10.1007/978-3-030-91327-4_48

19. Aghbalyan, S., Simonyan, V. 2022. Study of hardening and structure of maraging powder steel grade PS-H18K9M5TR (18%Ni+9%Co+5%Mo+1%Ti+1%Re+66%Fe). Scientific Herald of Uzhhorod University. Series "Physics", (52), 46-55. https://doi.org/10.54919/2415-8038.2022.52.46-55

20. Nussupbek, Z.T., Bekenov, T.N., Sattinova, Z.K., Beisenbi, M.A., Tassybekov, Z.T. 2023. Substantiation of methods for calculation of traction forces redistribution indicators on modular front and rear wheels of the vehicle (4X4). Transportation Engineering, 13, 100193. https://doi.org/10.1016/j.treng.2023.100193

21. Gierusz, W. 2016. Modelling the dynamics of ships with different propulsion for control purpose. Polish Maritime Research, 89(23), 31-36.

22. Guimarães, D. A. 2009. Digital Transmission: A Simulation-Aided Introduction with VisSim/Comm. New York: Springer Verlag. https://doi.org/10.1007/978-3-642-01359-1

23. Leshchev, V.A., Naydyonov, A.I. 2021. Dynamic Method for Determining Resonant Frequencies of Torsional Vibrations of a Ship's Propeller Shaft. A Scientific Look into the Future, 1(21), 15-26.

24. Gorb, S., Popovskii, A., Budurov, M. 2023. Adjustment of speed governor for marine diesel generator engine. International Journal of GEOMATE, 25(109), 125-132. https://doi.org/10.21660/2023.109.m2312

25. Califano, A. 2010. Dynamic loads on marine propellers due to intermittent ventilation. Trondheim: NTNU.

26. Kaplun, V., Chuenko, R., Makarevych, S. 2022. Investigation of energy parameters of a compensated asynchronous motor in the mode of repeated short-term starts. Machinery & Energetics, 13(3), 25-33. https://doi.org/10.31548/machenergy.13(3).2022.25-33

27. Ghaemi, M.H., Zeraatgar, H. 2022. Impact of propeller emergence on hull, propeller, engine, and fuel consumption performance in regular head waves. Polish Maritime Research, 29(4), 56-76. https://doi.org/10.2478/pomr-2022-0044

28. Kluczyk, M., Grządziela, A., Batur, T. 2022. Design and operational diagnostics of marine propellers made of polymer materials. Polish Maritime Research, 29(4), 115-122. https://doi.org/10.2478/pomr-2022-0049

29. Xiang, L., Yang, S.X., Gan, C.B. 2012. Torsional vibration of a shafting system under electrical disturbances. Shock and Vibration, 19, 1-11.

30. Quang, P.K., Hung, P.V., Cong, N.C., Tung, T.X. 2022. Effects of rudder and blade pitch on hydrodynamic performance of marine propeller using CFD. Polish Maritime Research, 29(2), 55-63. https://doi.org/10.2478/pomr-2022-0017

31. Fleischer, K.P. 1973. Untersuchungen über das Zusammenwirken von Schiff und Propeller bei teilgetauchten Propellern. Forschungszentrum des Deutschen Schiffbaus Bericht, 130(73), 291-308. [in German].